PMD compensation in a 2´40Gbit/s, 212km, CS-RZ polarization multiplexed transmission experiment

D. Sandel, F. Wüst, V. Mirvoda, R. Noé

Univ. Paderborn, FB 14/850, Warburger Str. 100, 33098 Paderborn, Germany, http://ont.upb.de/
(sandel@ont.upb.de, wuest@ont.upb.de, mirvoda@ont.upb.de, noe@upb.de)

Abstract: Endless polarization control is combined with PMD compensation in a polarization division multiplex experiment. Interchannel phase modulation allows to detect interference and pulse arrival time variations caused by polarization mismatch and PMD, respectively.

Introduction

Polarization division multiplex transmission (PolDM) /1-9/ has recently set fiber capacity records, with equal /7/ or unequal /4, 6/ frequencies of orthogonally polarized channels. The latter scheme is less PMD-tolerant than the former /5/. Based on equal per-channel bit rates both are less tolerant to PMD than standard transmission but no PMD compensation experiments have been reported for PolDM, to our knowledge. Moreover, we believe the mandatory endless polarization control for demultiplexing has been demonstrated so far only in our work /3/. One difficulty is that interchannel interference occurs proportional to a polarization mismatch angle. This can be exploited by interchannel phase modulation /5/. Here we go one step further and combine interference detection for endless polarization control with arrival time detection /8/ for PMD compensation in a 2×40Gbit/s, 212km, RZ PolDM transmission experiment.

Theory

Polarization division multiplex, where one bit modulates the horizontal and the other bit modulates the vertical electric field, is a quaternary modulation scheme (00, 01, 10, 11). The (11) symbol can have any polarization state among ±45° linear and right/left circular, depending on the phase shift between polarizations. We generate an interchannel differential phase modulation to vary the (11) symbol along the different possible polarization states. This depolarizes the transmitted signal.

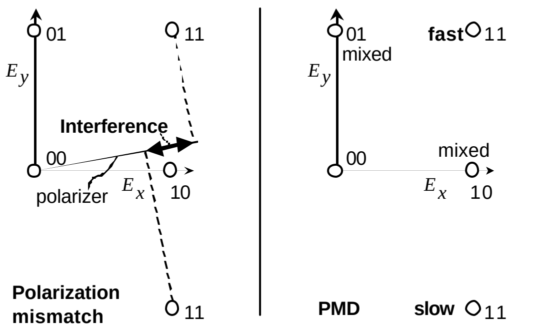

Figure 1: Interference and RZ arrival time modulation in the presence of interchannel phase modulation

Fig. 1 left shows the projection of (11) symbol fields onto a misaligned polarizer axis, the square of which is the received photocurrent carrying the interference. Fig. 1 right illustrates that the (11) symbol may travel along the fast or slow axis of a fiber with detrimental PMD. Here (01) and (10) symbols arrive with mixed polarizations.

In the receiver the depolarized light suffers PMD-induced arrival time variations $\Delta\hat{t}(t)$. The clock recovery PLL contains a phase detector that is part of the decision circuitry, a proportional-integral (PI) controller and a voltage-controlled oscillator (VCO). It tracks the arrival time variations as long as its bandwidth is large compared to the depolarization frequency. In that case the VCO input signal is proportional to the temporal derivative $d\Delta\hat{t}(t)/dt$. $\Delta\hat{t}(t)$ itself is obtained by integration. Its peak-to-peak value equals half the differential group delay (DGD).

For sinusoidal differential phase modulation, both interference signal and arrival time have Bessel spectra. We detect Bessel lines 2, 3 and 4 to obtain error signals which are independent of the static interchannel phase difference.

The simpler case of PMD occuring between horizontal and vertical axes would result in two undistorted, differentially delayed bit streams.

Experimental setup

A 2×40Gbit/s carrier-suppressed (CS) RZ PolDM transmission system was set up (Fig. 2). TX wavelength was 1541.6nm. A Mach-Zehnder modulator (CS-RZ) driven at 20GHz generated the 40GHz CS-RZ pulse stream. Pulse width was 13ps. 40Gbit/s data was imposed on the signal using another $LiNbO_3$ modulator. The signal was split, delayed in one arm by 224 bit durations (5.626ns) and recombined with orthogonal polarizations in a polarization beamsplitter (MUX). A frequency modulation (FM) with 240MHz peak-to-peak width and 417kHz fundamental frequency was applied to the TX laser to generate interchannel phase modulation with an index $h = 4.2$.

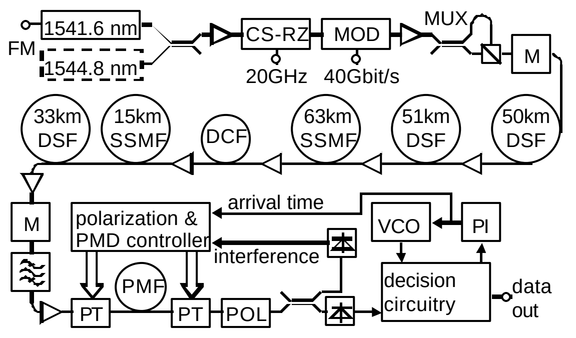

Figure 2: PolDM transmission with endless polarization control and PMD compensation

The signal was transmitted over a total of 134km of DSF, 78km of SSMF and additional DCF with -1000ps/nm of dispersion, using inline EDFAs. Powers lauched into the three DSF fiber sections were 0, +5 and +5dBm, respectively. In the receiver there were two polarization controllers (PC) with X-cut, Z-prop. $LiNbO_3$ devices, separated by PMF with a 4ps DGD section. The received signal was passed through a fiber polarizer. After electrical preamplification the 40Gbit/s signal was demultiplexed to 2.5Gbit/s where BER was measured on one randomly chosen sub-channel. For convenience, interchannel interference was measured in a separate control RX with low bandwidth. Normally one would tap this signal from the "cold" end of the photodiode. The interference detection signal was processed digitally and served to control the received polarization. The VCO input signal was processed similarly, but including an initial integration. The resulting signal served as an error signal for PMD compensation.

Results

Motorized polarization transformers (M) with 4 endlessly rotating fiber loops each were inserted before and after the transmission fiber, causing endless polarization changes. Speed was ~0.4rad/s on the surface of the Poincaré sphere plus faster harmonic content due to discontinuous stepper motor operation. In separate measurements, each of the polarization channels was transmitted error-free during 1h. Nevertheless simultaneous fiber handling was possible because finite polarization changes are much easier to track than endless ones. Eye diagrams back-to-back and after 212km are shown in Fig. 3. These were measured in an additional high-speed monitor diode (not shown in Fig. 2). Also depicted is the eye diagram which results if the link is operated only with polarization control but without PMD compensator.

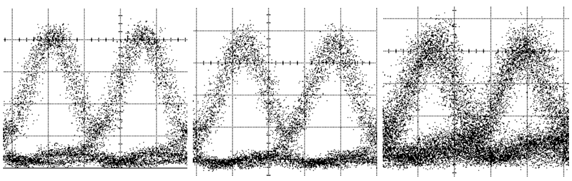

Figure 3: Eye diagrams back-to-back (left), after 212km with (middle) and without (right) PMD compensation

Then another laser (1544.8nm) was added to check for the effect of cross-phase modulation. A 400GHz frequency separation had to be chosen due to limited optical filter selectivity. The system was again operated error-free.

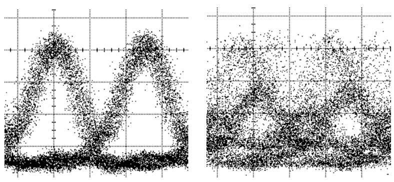

Figure 4: Worst case eye diagrams with 5.5ps of DGD compensated (left) or uncompensated (right)

Finally the transmission fiber was taken out and the system was operated back-to-back. The DGD of the PMD compensator was increased to 5.5ps. Between the two motorized polarization transformers another DGD section was inserted as a PMD emulator, with DGDs of 0, 2, 4, 5.5 and 6ps. Both for manual (seeking worst case) and motorized operation transmission was error-free. Fig. 4 left shows the eye pattern if the emulator with 5.5ps of DGD is set to worst case while the compensator cleans the eye. For comparison, in Fig. 4 right PMD compensation was switched off and only polarization control remained operational, with a total DGD near 5.5ps+5.5ps=11ps.

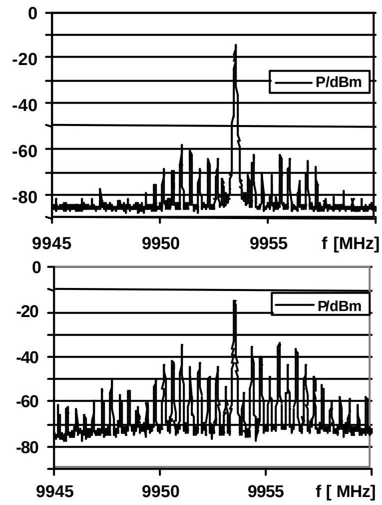

Figure 5: Prescaled clock spectra near 10GHz corresponding to Figure 4, with (top) and without (bottom) PMD compensation

Fig. 5 shows the corresponding clock spectra, prescaled to 10GHz. The side lines are due to PMD and are suppressed by >20dB if PMD compensation is operational. This suggests residual PMD was suppressed to <1ps.

PMD tolerance without PMD compensator (just polarization control) was also assessed: The system was operated error-free at 2ps of emulator DGD but not at≥4ps.

Conclusions

2×40Gbit/s CS-RZ polarization division multiplex transmission over 212km of fiber has been reported, for the first time with PMD compensation and endless polarization control. Interchannel phase modulation allowed to use detected interference as a polarization control error signal, while arrival time modulation served as a PMD compensation error signal. No extra optics or high-speed electronics are needed for error signal generation.

Acknowledgement

Partial support from Siemens ICN and Deutsche Forschungsgemeinschaft is gratefully acknowledged.

References

/1/ F. Heismann et al., WeP9.3, pp. 401-404, ECOC 1993, Montreux, Switzerland.

/2/ A.R. Chraplyvy et al., IEEE PTL 8 (1996) 1264

/3/ D. Sandel et al., ECOC 2000, Munich, Germany, Vol 3 pp. 103-105, Sept 3 – 7 2000

/4/ T. Ito et al., ECOC 2000, Munich, Germany, PDP 1.1, Sept 3 – 7 2000

/5/ S. Hinz et al., OSA Proc. OFC 2001, WM4

/6/ K. Fukuchi et al., OSA Proc. OFC 2001, PD24

/7/ S. Bigo et al., OSA Proc. OFC 2001, PD25

/8/ R. Noé et al., Proc. ECOC 2001, Amsterdam, NL, Sept. 30 - Oct. 4, 2001, Tu.A.3.4

/9/ N. Hecker et al., ECOC 2001, Mo.L.3.1, Amsterdam, Netherlands, Sept 30 – Oct 4 2001